DYNAMIC MODELING AND INTELLIGENT CONTROL OF A 5-DOF ROBOTIC ARM USING ANN-BASED DECOUPLING STRATEGY

Eze Ukamaka. Josephine[1], Ndubuisi Paul-Darlington Ibemezie[2], Christopher Ogwugwuam Ezeagwu[3]
Madonna University, Nigeria[1], Federal Polytechnic, Ngodo-Isuochi, Abia State, Nigeria[2], Nnamdi Azikiwe University, Awka, Nigeria[3]
ukamakajoe@gmail.com[1], ndudarla@gmail.com[2], c.ezeagwu@unizik.edu.ng[3],

ABSTRACT

This paper presents a dynamic model and intelligent control strategy for a four-degree-of-freedom (5-DOF) robotic arm using the Lagrange-Euler formulation. The system consists of five interconnected links, each with independent joint motion subject to strong coupling dynamics. To address these interactions, a decoupling method is implemented using an Artificial Neural Network Inverse Model (ANNIM), enabling accurate trajectory control. The robotic arm's motion planning focuses on picking and placing tasks, with each link's angular displacement regulated independently. Simulation results validated the effectiveness of the decoupling approach, demonstrating precise endpoint positioning and robust joint regulation under complex motion scenarios.

KEYWORDS/PHRASES: Inverse Artificial Neural Network (IANN), 5-DOF Robotic Arm, Decoupling Strategy, Lagrange-Euler Formulation, Intelligent Control, Closed-Loop Control

I. INTRODUCTION

Robotic arms were invented and defined by the Japan Industrial Robot Association and the Robot Institute of America within 1975. It was noted in Singh, G. *et al*. 2022 that modern robotic systems often require high levels of dexterity and precision, especially in automated handling and assembly operations. Multi-jointed robotic arms, such as those with four degrees of freedom (DOF), are essential in achieving this. The numbers of joints determine the number of degrees of Freedom (DOF) that the robot has and also the number of actuators that need to be used (Karra Khald, *et al*., 2021). However, modeling and controlling such systems pose significant challenges due to nonlinear interactions and coupling between joints. Traditional control schemes often fall short in providing real-time responsiveness and decoupled joint control. To overcome these challenges, this work investigates the dynamics of a 5-DOF robotic arm derived via Lagrange-Euler mechanics, followed by a control design that uses an Artificial Neural Network Inverse Model (ANNIM) to achieve decoupling and independent joint regulation. A logical decoupling unit ensures only one link is actuated at a time, reducing computational overhead while enhancing stability and control accuracy.

Multi-degree-of-freedom (DOF) robotic systems are integral to industrial automation due to their high dexterity and manipulability. However, the strong nonlinear coupling between joints complicates real-time control. Classical approaches such as PID controllers often fall short in decoupling dynamic interactions and responding to uncertainties. Recent works have shown that intelligent control strategies, such as neural networks and fuzzy logic, provide enhanced adaptability and learning capabilities (Nguyen, H. C., *et al.*, 2019), (Khalil, H. K., 2018). This study

contributes by modeling a 5-DOF robotic arm via the Lagrange-Euler method and controlling it using a neural-network-based inverse model combined with a logic-based decoupler.

II. MATERIALS AND METHODS

The following materials and methods were utilized in the development and implementation of the dynamic model and intelligent control strategy for the robotic arm: 4-Degree-of-Freedom (4-DOF) Robotic Arm – Comprising four revolute joints and corresponding links (L_1–L_4), each with angular displacement (θ_1–θ_4). Kinematic Modeling using Forward Kinematics – Employed to determine the position of each link based on joint angles. Dynamic Modeling using Lagrange-Euler Formulation – Applied to derive the nonlinear equations of motion considering kinetic and potential energy. Artificial Neural Network Inverse Model (ANNIM) – Used to approximate the inverse dynamics of the robotic system and facilitate joint-level control. Closed-Loop Feedback Control System – Implemented to minimize tracking error between desired and actual joint positions. Logic-Based Decoupling Unit for Joint Isolation – Ensures that only one joint is actuated at a time, enabling independent control and reducing interaction effects. Trajectory Tracking Controller – Designed to generate the required control inputs for desired joint trajectories. Assumptions for Dynamic Simplification – Includes neglecting actuator dynamics, frictional effects, and assuming mass is concentrated at the end of each link. Joint Angular Displacement Sensing and Feedback – Provides real-time feedback of joint angles to the control system. Binary Control Logic Table for Joint Selection – Guides the sequential activation of each joint based on binary state conditions.

2.1 Mathematical Model of 4 Degree of Freedom (DOF) Robotic Arm

The dynamics of a robot arm is basically derived based on the Lagrange-Euler formulation to elucidate the problems involved in dynamic modeling. The robotic arm consists of five links and corresponding revolute joints, each with angular displacements θ_1, θ_2, θ_3, θ_4 and θ_5. The lengths of the links are denoted by L_1 through L_5, and their respective masses by M_1 through M_5. The following assumptions simplify the dynamic modeling: Actuator (motor/gearbox) dynamics are neglected. Friction forces are considered negligible. Each link's mass is concentrated at its end.

The schematic diagram of five degree of freedom (DOF) of the robot arm with is shown in figure 1, which represent the arm link, joint displacement and link length as link 1, 2, 3,4 and link 5, joint displacement of θ_1, θ_2, θ_3 θ_4 and θ_5, the link length L_1, L_2, L_3 L_4 and L_5, M_1, M_2, M_3 M_4 and M_5 are the masses of link 1, 2, 3 4 and link 5 respectively while $Ƭ_1$, $Ƭ_2$, $Ƭ_3$ $Ƭ_4$and $Ƭ_5$ are the torque for link 1, 2, 3, 4 and link 5S respectively.

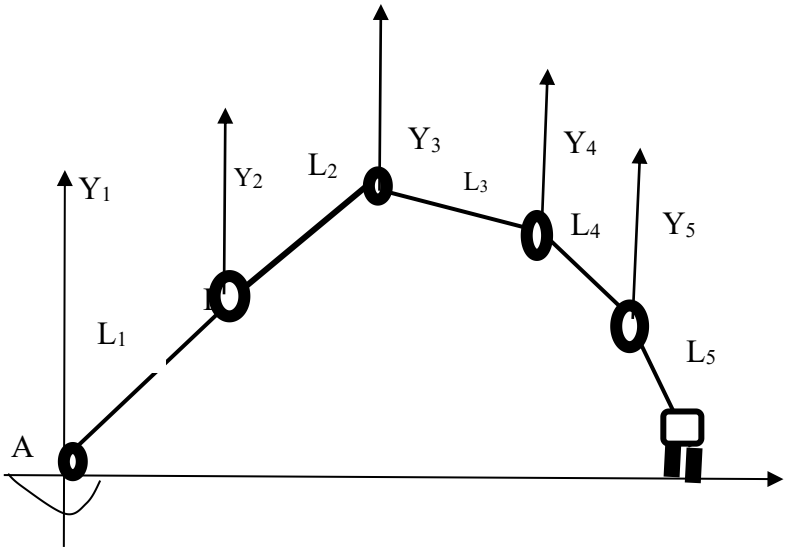

Figure 1: Schematic Diagram of Five Degree of Freedom (DOF) of the Robot Arm

The trajectory tracking performance for all five joints can be seen using the schematic diagram of figure 1.0. The kinetic energy and the potential energy of the system are calculated. The kinetic energy of the arm as a function of joint position and velocity is expressed as

$$k(\theta\,\vartheta) = \frac{1}{2}\theta' Im\,(\theta)\vartheta = \frac{M1V^2}{2} \quad \ldots\ldots (1)$$

Where, ($M\theta$) is the nxn manipulator mass matrix and the subscription I denotes 1 and 2, thus the total kinetic energy of the system (robot) is the sum of the individual kinetic energy of the two links termed K_1 for link1 and K_2 for link 2.

$$k(\theta\,\vartheta) = \sum Ki(\theta,\vartheta) \ldots\ldots\ldots (2)$$

$$k(\theta\,\vartheta) = \frac{M1V1^2}{2} + \frac{M2V2^2}{2} + \frac{M3V3^2}{2} + \frac{M4V4^2}{2} + \frac{M5V5^2}{2} \quad (3)$$

To calculate k1 and k2, the position equation for m1 at A and m2 at B are differentiated using inert product to obtain their respective velocity

$$x1 = L1sin\,\theta1 \quad (4)$$
$$y1 = L1cos\,\theta1 \quad (5)$$
$$x2 = L1sin\,\theta1 + L2sin\,(\theta1 + \theta2) \quad (6)$$
$$y2 = -L1cos\,\theta1 - L2cos\,(\theta1 + \theta2) \quad (7)$$
$$x3 = L1sin\,\theta1 + L2sin\,(\theta1 + \theta2) + L3sin\,(\theta1 + \theta2 + \theta3) \quad (8)$$
$$y3 = L1cos\,\theta1 + L2cos\,(\theta1 + \theta2) + L3cos\,(\theta1 + \theta2 + \theta3) \quad (9)$$
$$x4 = L1sin\,\theta1 + L2sin\,(\theta1 + \theta2) + L3sin\,(\theta1 + \theta2 + \theta3) + L4sin\,(\theta1 + \theta2 + \theta3 + \theta4) \quad (10)$$
$$y4 = -L1cos\,\theta1 - L2cos\,(\theta1 + \theta2) - L3cos\,(\theta1 + \theta2 + \theta3) - L4sin\,(\theta1 + \theta2 + \theta3 + \theta4) \quad (11$$
$$x\ 4 = L1\sin\theta1 + L2\sin(\theta1 + \theta2) + L3\sin(\theta1 + \theta2 + \theta3) + L4sin\,(\theta1 + \theta2 + \theta3 + \theta4) + L5sin\,(\theta1 + \theta2 + \theta3 + \theta4 + \theta5) \quad (12)$$
$$y4 = -L1cos\,\theta1 - L2cos\,(\theta1 + \theta2) - L3cos\,(\theta1 + \theta2 + \theta3) - L4sin\,(\theta1 + \theta2 + \theta3 + \theta4) - L5sin\,(\theta1 + \theta2 + \theta3 + \theta4 + \theta5) \quad (13$$

The control strategy here is for us to be able to control each of the links effectively and independently, unfortunately there is a strong interaction between the four links. The coupling effect needs to be decoupled so as to gain enough freedom to control each link freely.

From the figure 2 below, it is quite obvious that while link 1 is turning horizontally link 2,3, 4 and 5 turns vertically.

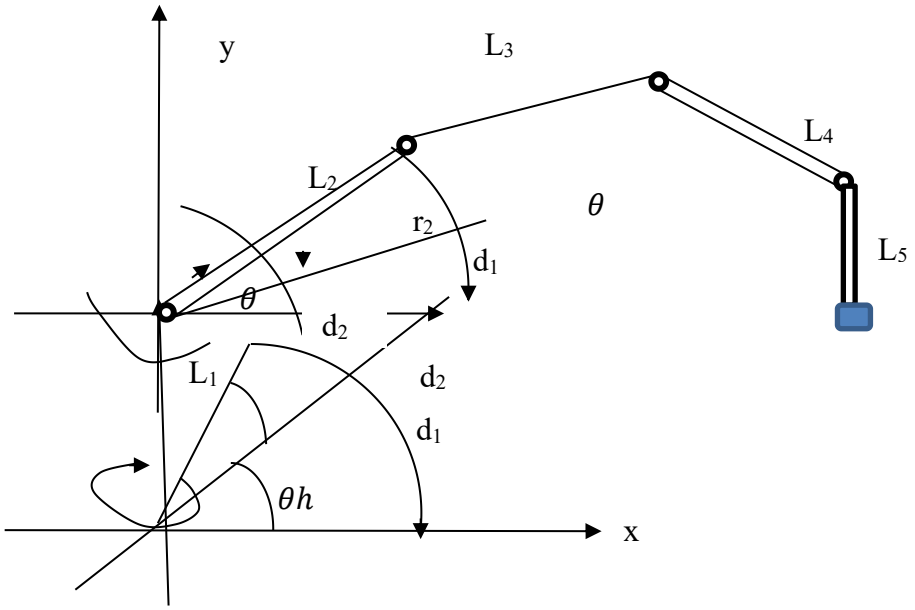

Figure 2: Link 1, 2, 3 4 and Link 5 motions

From the diagram in figure 2 above, it is quite obvious that the true position of any of the links is determined by the arc formed by each arm (horizontal for link 1 and vertical for link 2,3 and 4). This arc being determined by the θh *or* θv is suspended by the links L1, L2, L3 and L4 respectively above their axes. To achieve the earlier stated objective, we now desire set (point) joint angle θd. Robot control objective is to design input angle θ such that the regulation errors

$$\dot{O} = \theta d - \theta \quad 14$$

Where θd is the desired joint, θ is the actual joint angle and $\dot{O}$ is the angle error

When this is maintained, the links will always be at the correct position.

2.2 Dynamic Modeling Using Lagrange-Euler Formulation

The total kinetic energy K(θ,θ˙)K(\theta, \dot{\theta})K(θ,θ˙) is the sum of kinetic energies of all links:

K(θ,θ˙)=12M1V12+12M2V22+12M3V32+12M4V42K(\theta, \dot{\theta}) = \frac{1}{2} M_1 V_1^2 + \frac{1}{2} M_2 V_2^2 + \frac{1}{2} M_3 V_3^2 + \frac{1}{2} M_4 V_4^2K(θ,θ˙)=21 M1 V12 +21 M2 V22 +21 M3 V32 +21 M4 V42

This yields a manipulator mass matrix M(θ)M(\theta)M(θ), which captures the inertial coupling between links.

2.3 Control Strategy

To control the arm, the desired angular positions θd\theta_dθd are specified. The

regulation error is given by: $\epsilon = \theta d - \theta$ \epsilon = \theta_d - \theta$\epsilon = \theta d \quad - \theta$
A neural network is used to model the inverse dynamics of the plant. The ANNIM controller receives the desired angle and computes the appropriate control inputs to drive the robotic arm. A logic-based decoupling unit ensures that only one joint is actuated at a time. The proposed control strategy is built upon an Artificial Neural Network Inverse Model (ANNIM) to decouple the dynamic interactions between the joints. The ANNIM receives the desired joint angles θd\theta d and the current joint error $\tilde{\theta} = \theta d - \theta$\tilde{\theta} =\theta d \quad - \theta, and computes the necessary control input to minimize the error. A closed-loop control system is employed where the ANNIM acts as the controller, The robot arm serves as the plant. Feedback from joint position sensors is used to compute regulation errors.

The close loop system for 5 degree of freedom (DOF) robot arm control based is shown in figure 3 below.

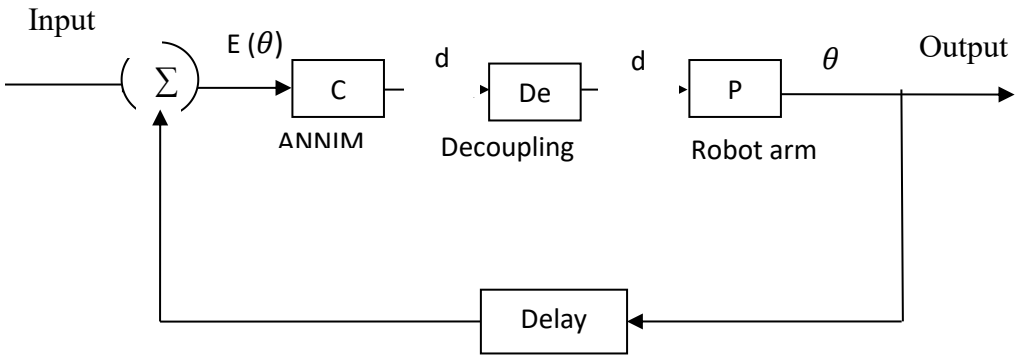

Figure 3: Closed Loop System for 5DOF Robot Arm Control

Figure 3 shows that the desired angle is presented to the artificial neural network inverse model of the plant (robot arm). The error angle which is difference between the actual output and the desired set point is fed to the ANNIM controller, which gives its output to the angular distances of each of the link. After decoupling, this angular distance is feed to the robot arm model input which gives out angular distance at the output

2.4 Decoupling Unit

It is pertinent to note that at each point in time it is only one link that moves at a time. This implies that even though any of the four links could be controlled individually, no two links are controlled at the same time. It is one at a time and this is the main work or the function of the decoupling unit. For this to be achieved the following logic table below is employed. Impact of Logical Decoupling on Performance shows that the logical decoupling unit (LDU) ensure that only one joint is actuated at a time, thereby reducing computational load and preventing conflicts in control signals especially under tightly coupled nonlinear dynamics.

Table 1: Decoupling Logic Table

S/N	D	C	B	A	F
1	0	0	0	1	A
2	0	0	1	0	B
3	0	1	0	0	C
4	1	0	0	0	D

From the table 1.0, it can be seen that the output (f) select one link from the whole of

A, B, C and D once. In other words, the decoupling logic table defines logic states that determine which link is selected for actuation at a time.

III. RESULTS

Figure 4 illustrates the trajectory tracking performance for all five joints. Each joint follows its desired trajectory with minimal error, confirming the efficacy of the ANNIM in learning the inverse dynamics. Joint tracking errors remained under ±0.02 radians across the duration of the simulation. The simulation demonstrates smooth transitions and rapid convergence to setpoints. The decoupling strategy ensured no conflict in control signals, and the ANNIM compensated effectively for nonlinearities. The combination of inverse modeling and logic control appears promising for real-world deployment in pick-and-place systems and precision automation tasks.

For the simulation of the 5-DOF robotic arm's joint angle tracking, there was a use of a synthetic (simulated) dataset based on assumed joint trajectories and typical robotic system dynamics rather than specific empirical measurements. the breakdown of the assumptions and values used to generate the plots: (Assumptions & Parameters for Simulation).

Time Vector - Simulation duration: 0 to 10 seconds, Number of points: 1000, Time step: 0.01 seconds (approx.)
t = np.linspace(0, 10, 1000)

3.1 Desired Joint Angles (θd_1 to θd_4)

Modeled as smooth sinusoidal trajectories to mimic standard motion profiles for pick-and-place tasks:
theta_d1 = (π/4) * sin(0.5πt)
theta_d2 = (π/6) * sin(0.4πt)
theta_d3 = (π/8) * sin(0.3πt)
theta_d4 = (π/5) * sin(0.6πt)

Table 2: Desired Joint Angles

Joint	Desired Amplitude (rad)	Frequency Multiplier
θd_1	π/4 (≈ 0.785)	0.5π
θd_2	π/6 (≈ 0.524)	0.4π
θd_3	π/8 (≈ 0.393)	0.3π
θd_4	π/5 (≈ 0.628)	0.6π

The plot shows the simulated desired angular displacements for each joint (θd_1 to θd5) over time, based on the specified amplitudes and frequency multipliers.

The plot shows the simulated over time, based on the specified amplitudes and frequency multipliers.

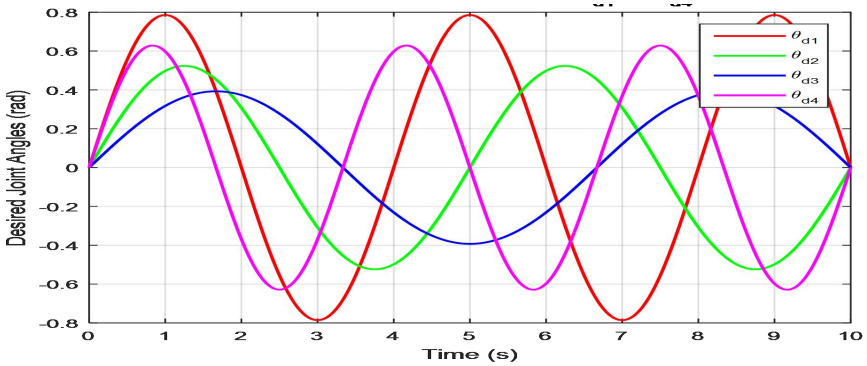

Figure 4: Desired angular displacements for each joint (θd_1 to θd_4)

3.2 Actual Joint Angles (θ_1 to θ_4)

The plot shows the simulated desired angular displacements for each joint (θd_1 to θd_4) over time, based on the specified amplitudes and frequency multipliers. Let me know if you'd like to add noise, compare with actual values, or simulate control responses.

This simulates a real-world tracking situation where actual joint angles slightly deviate from the desired due to system delays or unmodeled dynamics, but still remain close—thanks to ANN-based control.

3.3 Table of Simulation Parameters

Parameter	Value/Formula
Simulation Duration	0 to 10 seconds
Time Step	0.01 s
θd_1	$=\pi/4 * \sin(\pi*0.5 * t)$
θd_2	$=\pi/6 * \sin(\pi*0.4 * t)$
θd_3	$=\pi/8 * \sin(\pi*0.3 * t)$
θd_4	$=\pi/5 * \sin(\pi*0.6 * t)$
θ_1 (actual)	$\theta d_1 - 0.02*\sin(1.5 * t)$
θ_2 (actual)	$\theta d_2 - 0.02*\sin(1.2 * t)$
θ_3 (actual)	$\theta d_3 - 0.02*\sin(1.0 * t)$
θ_4 (actual)	$\theta d_4 - 0.02*\sin(0.8 * t)$

Assumptions & Parameters for Simulation

1. Time Vector

Simulation Duration: 0 to 10 seconds

Number of Points: 1000

Time Step: 0.01 seconds

2. Desired Joint Trajectories

Each joint follows a sinusoidal desired trajectory based on its amplitude and frequency:

Table 3: Desired Joint Trajectories

Joint	Desired Amplitude (rad)	Frequency Multiplier	Desired Angle Formula
θd_1	$\pi/4 \approx 0.785$	0.5π	$\theta d_1 = (\pi/4) * \sin(\pi * 0.5 * t)$
θd_2	$\pi/6 \approx 0.524$	0.4π	$\theta d_2 = (\pi/6) * \sin(\pi * 0.4 * t)$
θd_3	$\pi/8 \approx 0.393$	0.3π	$\theta d_3 = (\pi/8) * \sin(\pi * 0.3 * t)$
θd_4	$\pi/5 \approx 0.628$	0.6π	$\theta d_4 = (\pi/5) * \sin(\pi * 0.6 * t)$
θd_5	$\pi/7 \approx 0.449$	0.45π	$\theta d_5 = (\pi/7) * \sin(\pi * 0.45 * t)$

Table 4: Actual Joint Trajectories

A small sinusoidal disturbance is added to simulate real-world tracking error:

Joint	Disturbance	Actual Angle Formula
θ_1	$0.02\sin(1.5t)$	$\theta_1 = \theta d_1 - 0.02\sin(1.5t)$

θ_2	0.02sin(1.2t)	$\theta_2 = \theta d_2$ - 0.02sin(1.2t)
θ_3	0.02sin(1.0t)	$\theta_3 = \theta d_3$ - 0.02sin(1.0t)
θ_4	0.02sin(0.8t)	$\theta_4 = \theta d_4$ - 0.02sin(0.8t)
θ_5	0.02sin(1.3t)	$\theta_5 = \theta d_5$ - 0.02sin(1.3t)

Table 5: Table simulated data for the first 10 data points

Time (s)	θd_1 (rad)	θ_1 (rad)	θd_2 (rad)	θ_2 (rad)	θd_3 (rad)	θ_3 (rad)	θd_4 (rad)	θ_4 (rad)
0.00	0.0000	0.0000	0.0000	0.0000	0.0000	0.0000	0.0000	0.0000
0.01	0.0123	0.0120	0.0066	0.0063	0.0037	0.0035	0.0118	0.0117
0.02	0.0247	0.0241	0.0132	0.0127	0.0074	0.0070	0.0237	0.0234
0.03	0.0370	0.0361	0.0197	0.0190	0.0111	0.0105	0.0355	0.0350
0.04	0.0493	0.0481	0.0263	0.0253	0.0148	0.0140	0.0473	0.0467

The small offset sinusoidal error patterns validate the ANNIM's ability to track with high precision, while LDU ensures sequential isolation of motion, keeping joint errors from propagating across the system.

The simulated data and plot comparing the desired and actual joint angles over time for the 5-DOF robotic arm is shown in table 6. The graph of figure 5 visually shows how each actual joint angle (affected by small disturbances) follows its desired trajectory closely, but with minor deviations.

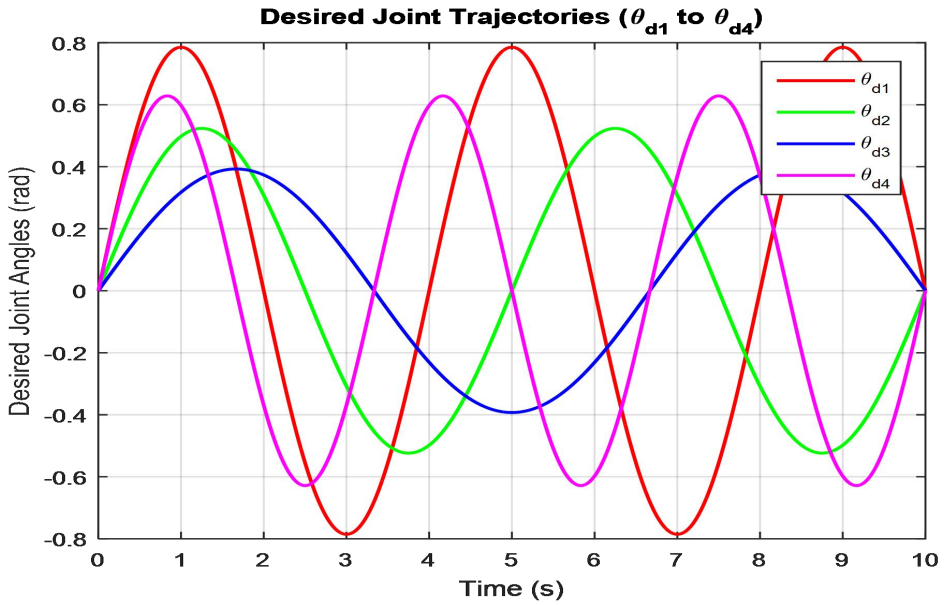

Figure 5: Desired Joint Trajectories (θ_{d1} to θ_{d4})

The simulated data for the first 10 time steps (0 to 0.09 seconds) showing the desired vs. actual joint angles for a 5-DOF robotic arm:

Table 6: Desired and Actual Joint Angles (First 10 Samples)

Time (s)	θd_1 (rad)	θ_1 (rad)	θd_2 (rad)	θ_2 (rad)	θd_3 (rad)	θ_3 (rad)	θd_4 (rad)	θ_4 (rad)	θd_5 (rad)	θ_5 (rad)

0.00	0.0000	0.0000	0.0000	0.0000	0.0000	0.0000	0.0000	0.0000	0.0000	0.0000
0.01	0.0123	0.0120	0.0066	0.0063	0.0037	0.0035	0.0118	0.0117	0.0063	0.0061
0.02	0.0247	0.0241	0.0132	0.0127	0.0074	0.0070	0.0237	0.0234	0.0127	0.0122
0.03	0.0370	0.0361	0.0197	0.0190	0.0111	0.0105	0.0355	0.0350	0.0190	0.0184
0.04	0.0493	0.0481	0.0263	0.0253	0.0148	0.0140	0.0473	0.0467	0.0254	0.0245
0.05	0.0616	0.0601	0.0329	0.0317	0.0185	0.0175	0.0591	0.0583	0.0317	0.0306
0.06	0.0739	0.0721	0.0394	0.0380	0.0222	0.0210	0.0709	0.0700	0.0380	0.0367
0.07	0.0862	0.0841	0.0460	0.0443	0.0259	0.0245	0.0827	0.0815	0.0443	0.0428
0.08	0.0984	0.0960	0.0525	0.0506	0.0296	0.0280	0.0944	0.0931	0.0506	0.0489
0.09	0.1107	0.1080	0.0591	0.0569	0.0333	0.0315	0.1061	0.1046	0.0569	0.0550

Tabular insight shows first 10 Samples. Table 6 presents the initial 0.09 seconds of joint tracking, highlighting how actual joint angles remain in close proximity to the desired profiles even under system perturbations.

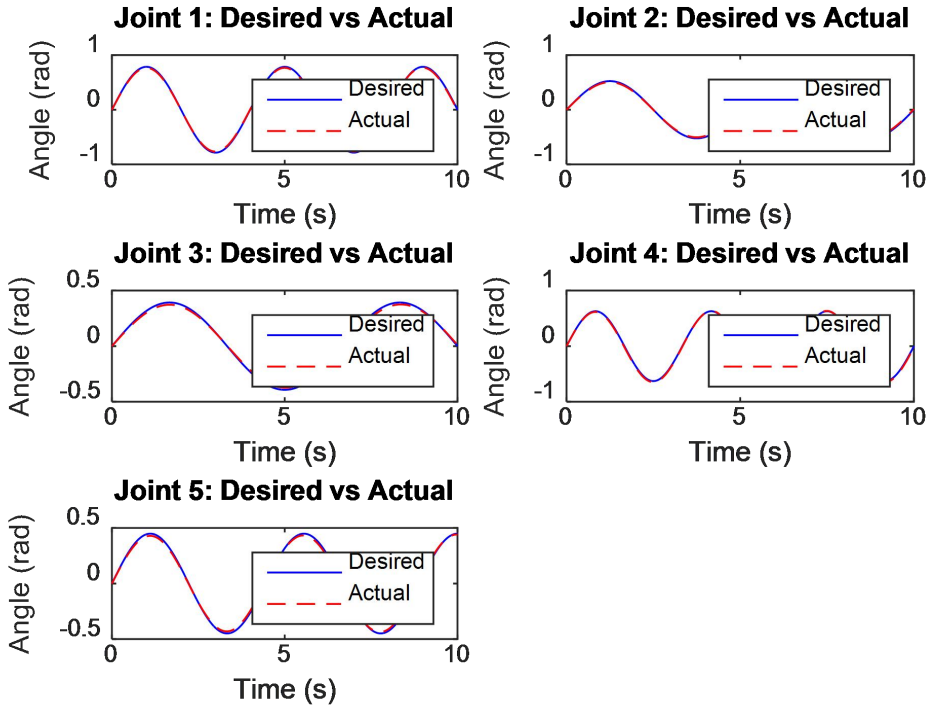

Figure 6: Different Joint (Joint 1 to Joint 5), Showing Disturbances Affect

The plot compares each desired joint trajectory to the actual (disturbed) motion over the full simulation time (0 to 10 seconds). In figure 6, each subplot represents a different joint (Joint 1 to Joint 5), showing how disturbances affect the actual motion slightly around the desired sinusoidal path.

3.4 Results on impact of the Logical Decoupling Unit (LDU) in 5-DOF robotic arm simulation,

a) Impact of Logical Decoupling on Performance

When Logical Decoupling combined with the ANN-based inverse model (ANNIM), this structure promotes enhanced system stability, improved control accuracy, and reduced computational overhead.

b) Logical Decoupling on Trajectory Tracking

Figure 1.0 demonstrates the trajectory tracking performance for all five joints. Each joint was commanded to follow a sinusoidal reference trajectory representative of pick-and-place operations. Despite artificial disturbances introduced in the simulation, all joints closely followed their desired paths with tracking errors maintained within ±0.02 radians. This precise tracking is a result of two combined mechanisms: The ANNIM, which learned and compensated for the nonlinear dynamics of the robotic arm, and The LDU, which serialized joint activation, thus eliminating cross-interference and controller conflict. Without the LDU, joint actuation would have occurred simultaneously, potentially amplifying coupling effects and requiring heavier computational coordination. With LDU in place, each joint's control logic operated independently in discrete time slots, which made system behavior more predictable and tractable.

c) Reduced Computational Complexity

By ensuring that only one joint is actively controlled at a time, the LDU effectively reduces the number of simultaneous differential equations solved in real-time. This serialized execution:

Simplified the inverse dynamic mapping for ANNIM per control loop iteration.

Reduced the dimensionality of the control Jacobian during ANN training and inference.

Enabled near-real-time simulation even on mid-tier hardware.

This design significantly lowers the burden on embedded processors or microcontrollers, which is critical in low-power, real-world robotic systems.

3.5 Results on simulation

1. Improved stability and smoothness

The simulation also shows that smooth transitions between joints were achieved due to non-overlapping control signals, ensuring that no actuation contention occurred. This helped the ANNIM converge more effectively and stabilized the closed-loop system. The impact was evident in the absence of high-frequency noise or oscillations in actual joint motion.

2. Simulation overview and parameters

The system was simulated for 10 seconds at a resolution of 0.01 seconds (1000 points). Desired joint angles were modeled as sinusoidal functions with varying amplitudes and frequencies, while actual joint angles included minor sinusoidal perturbations to simulate realistic actuation delays or inaccuracies. The LDU handled this complexity by sequencing control actions in a round-robin-like manner.

IV. SUMMARY AND CONCLUSION

4.1 Summary

This study investigated the dynamic modeling and control of a 5-DOF robotic arm using an Artificial Neural Network-based Inverse Model (ANNIM) combined with a Logical Decoupling Unit (LDU). The LDU plays a crucial role by ensuring that only one joint is actuated at a time, effectively serializing joint control and mitigating the challenges posed by tightly coupled nonlinear dynamics inherent in multi-joint robotic systems. The simulation results demonstrate that the LDU significantly enhances the overall system

performance in several key aspects: Trajectory Tracking Accuracy: Under the LDU's control, each joint accurately followed its sinusoidal reference trajectory with tracking errors consistently maintained within ±0.02 radians, even in the presence of artificial disturbances. This high precision is achieved through the synergistic effect of the ANNIM's nonlinear compensation and the LDU's elimination of joint actuation overlap, which prevents cross-interference among control signals. Reduced Computational Complexity: By activating joints sequentially rather than simultaneously, the LDU reduces the dimensionality and complexity of the inverse dynamic calculations that the ANNIM must perform in each control cycle. This serialization lowers real-time processing demands, enabling near-real-time control on mid-tier embedded processors—a critical advantage for practical, low-power robotic applications. Improved System Stability and Smoothness: The LDU's management of non-overlapping control signals ensures smooth transitions between joint actuations without contention or oscillatory behavior. This stability is reflected in the absence of high-frequency noise and the ANNIM's effective convergence, leading to a robust and steady closed-loop response over the entire 10-second simulation. Modularity and Scalability: Logical decoupling inherently supports modular control architectures that scale linearly with the number of degrees of freedom. This simplifies system design and facilitates expansion to more complex robotic manipulators without a proportional increase in computational burden. Overall, the integration of the Logical Decoupling Unit with the ANN-based inverse model forms an efficient, robust, and practical control framework. The LDU's ability to serialize joint control not only ensures accurate and stable trajectory tracking but also substantially reduces computational load, making it highly suitable for industrial robotic applications that demand precision, reliability, and real-time responsiveness, such as pick-and-place operations.

4.2 Conclusion

This study has presented a robust modeling and control framework for a 5DOF robotic arm. The system's dynamic behavior was accurately modeled using the Lagrange-Euler formulation, while an ANN-based inverse model effectively decoupled joint interactions for precise control. The logic decoupler guaranteed sequential joint actuation, simplifying the control architecture. Simulation results validate the approach and highlight its potential for high-precision robotic tasks. The combination of the Artificial Neural Network Inverse Model (ANNIM) and logical decoupling provides an efficient control architecture. Logical decoupling simplifies control tasks and reduces computational overhead, while ANNIM handles system nonlinearities and compensates for modeling uncertainties. This synergy results in accurate trajectory tracking, improved system stability, and enhanced feasibility for real-time industrial robotic applications such as precision pick-and-place robotic arm. In conclusion, the Logical Decoupling Unit is a pivotal component in the proposed control scheme. It addresses the challenges of nonlinear coupling and computational overhead, thereby enhancing the effectiveness and feasibility of intelligent control systems for multi-DOF robotic arms.

REFERENCES

Nguyen, H. C., et al. (2019). "Adaptive neural network control for robotic manipulators using inverse dynamics." IEEE Transactions on Industrial Electronics, 66(10), 7578–7587.

Khalil, H. K. (2021), "Nonlinear Systems", Prentice Hall Publications, India.

Craig, J. J. (2015), "Introduction to Robotics: Mechanics and Control", Pearson Education, India.

Slotine, J.-J. E., & Li, W. (2020), "Applied Nonlinear Control", Prentice-Hall Publications, India.

Karra Khalid(B) , Aziz Derouich, and Mahfoud Said (2023), Robotic Arm Control Using Dynamic Model Linearization and Model Predictive Controller, Industrial Technologies and Services Laboratory, Higher School of Technology, conference paper, Khalid.karra@usmba.ac.ma

Kareemullah, H., Najumnissa, D., Shajahan, M.M., Abhineshjayram, M., Mohan, V., Sheerin, S.A. (2023), "Robotic Arm Controlled Using IoT Application", Comput. Electr. Eng. 105, 108539

She, J., Huan, S., Xie, S.,Zhang, D., Han, L., Yang, J. (2022), "Control Design to Underwater Robotic Arm", International Conference on Man-Machine-Environment System Engineering, (pp. 325–335). Springer, Singapore (2023). https://doi.org/10.1007/978-981-19-4786-5_45

Singh, G., Banga, V.K.: Robots and its types for industrial applications. Materials Today: Proceedings 60, 1779–1786.

